DS-Compatible Log-Linear Reliability with KL-Prox EM: Monotone Ascent, Identifiability, and Generalization

Shiva Koreddi SHIVA.KOREDDI@WNCO.COM
Southwest Airlines
Sravani Sowrupilli SOWRUPILLI.SRAVANI@GMAIL.COM

Editor: Proceedings of ALT 2026

Abstract

We study *context-conditioned* reliability in Dawid–Skene (DS) models and propose a DS-compatible parameterization in which a log-linear correction to confusion logits is softmax-renormalized *over reported labels*, yielding valid, interpretable confusion matrices conditioned on covariates. We derive a *KL-proximal* (mirror-descent) update for confusion matrices that warm-starts at DS and provably yields *monotone ascent* of a standard EM surrogate. Under diagonal-dominance at warm start and mild covariate excitation, we prove *identifiability up to permutation*; for the correction head we give a finite-sample *generalization* bound of order $O(\sqrt{d\log(dK)/n})$ via Rademacher complexity. The formulation drops into vanilla EM, preserves DS interpretability, and supports physics-inspired priors (e.g., monotonicity) without breaking guarantees. Empirical validation on multi-agent label fusion confirms monotone convergence and calibration improvements with minimal overhead.

Keywords: truth discovery; Dawid–Skene; EM; mirror descent; proximal methods; identifiability; generalization bounds; multi-agent perception

1. INTRODUCTION

Truth discovery (TD) is the task of inferring an unobserved *true* label for each item when we only observe multiple *noisy* categorical reports from different labelers (annotators, sensors, or models). In a classification setting, each labeler can be viewed as a predictor that outputs a label $y_{n,a}$ together with contextual metadata $x_{n,a}$ (e.g., range, bearing, latency), and the goal is to *aggregate* these heterogeneous predictions into a single calibrated posterior over the latent truth z_n.

A canonical probabilistic model for TD is the Dawid–Skene (DS) model (5), which treats z_n as a latent variable and parameterizes each labeler a by a confusion matrix Π_a describing $P(y_{n,a} \mid z_n, a)$. DS estimates $(\{\Pi_a\}, \pi)$ by maximum likelihood via EM. In real deployments, however, noise is frequently *state-dependent*: reliability varies with instance, labeler, and context. We seek a DS-compatible way to encode such dependence *without* sacrificing interpretable confusion semantics or EM-style inference guarantees.

Problem to be solved (MLE on a DS-compatible class). Given observations $\{(y_{n,a}, x_{n,a})\}$ with $y_{n,a} \in \{1, \dots, K\}$, covariates $x_{n,a} \in \mathbb{R}^d$, and observer sets S_n, we consider a parametric family Θ in which the noise model is a *context-conditioned confusion matrix* $\tilde{\Pi}_a(x)$ and the joint model factorizes as $p(z_n = k) = \pi_k$ and $p(\{y_{n,a}\}_{a\in S_n} \mid z_n = k, \{x_{n,a}\}) = \prod_{a\in S_n} \tilde{\Pi}_{a,y_{n,a},k}(x_{n,a})$. Our estimator is the maximum likelihood estimator (MLE)

$$\hat{\theta} \in_{\theta\in\Theta} \sum_{n=1}^{N} \log\left(\sum_{k=1}^{K} \pi_k \prod_{a\in S_n} \tilde{\Pi}_{a,\, y_{n,a},\, k}(x_{n,a})\right), \tag{1}$$

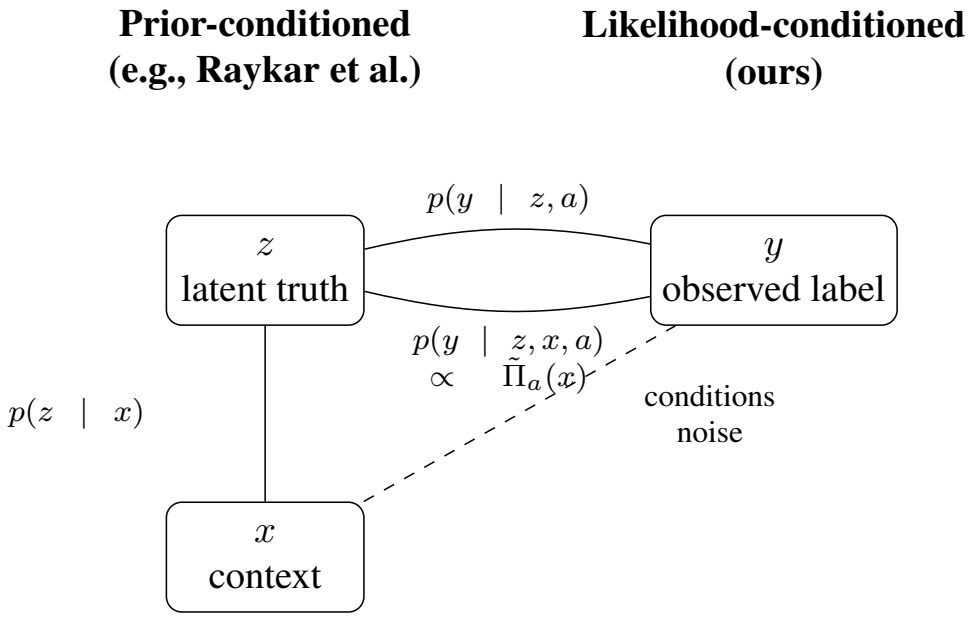

Figure 1: Where covariates enter DS-style models: conditioning the prior $p(z \mid x)$ captures instance "difficulty"; conditioning the likelihood $p(y \mid z, x, a)$ captures context-dependent *reliability*.

where $\theta = (\pi, \{\Pi_a\}, \phi)$ parameterizes $\tilde{\Pi}_a(\cdot)$ (Section 3). We optimize (1) with an EM algorithm whose M-step uses a KL-proximal (mirror-descent) update, yielding stable monotone ascent.

Motivating example (multi-agent label fusion). Three agents observe the same object at an urban intersection: a lead vehicle is near and head-on; a follower is farther and partially occluded; a roadside unit (RSU) is clear but time-lagged. Per-agent error rates change with range, bearing, occlusion, and latency (4; 15; 9). A label-fusion module must combine these heteroskedastic, asynchronous reports into a single calibrated posterior fast enough for planning.

Why static DS is insufficient. Static Π_a averages over diverse observation conditions, over-trusting far/off-axis or stale reports and miscalibrating posteriors even when top-1 accuracy is unchanged. Heuristic geometry weights inside DS often break normalization and destabilize EM. Discretizing context via binning fragments data; fully neural confusion parameterizations can obscure conditional semantics and oscillate during training (12; 14; 18).

Likelihood- vs. prior-conditioning. A recurring point of confusion is *where* covariates enter the latent-variable model. Instance-aware DS extensions such as Raykar et al. (12) primarily condition the *prior* $p(z \mid x)$ ("is this item difficult?"), while keeping annotator noise global. In contrast, our goal is to capture *context-dependent reliability*: we condition the *likelihood* $p(y \mid z, x, a)$ through a context-conditioned confusion matrix $\tilde{\Pi}_a(x)$ ("is annotator a reliable *here*?"), enabling complementary strengths (e.g., one agent reliable at short range, another at long range) to be expressed without losing DS semantics.

Design desiderata. The upgrade should (i) be plug-in and preserve DS *conditional probability semantics* $P(y|z, x)$; (ii) enforce valid confusion matrices by construction; (iii) train stably with *monotone ascent*; (iv) allow weak priors (e.g., range monotonicity); (v) degrade gracefully to DS when covariates are weak; and (vi) maintain $O(K)$ per-edge cost.

One-sentence approach. Keep each agent's DS confusion Π_a as an anchor; learn a small log-linear correction $\alpha(x)$ in logit space from context x (range, bearing, latency, identity); renormalize *over reported labels* (rows) by softmax to get valid context-conditioned confusion matrices $\tilde{\Pi}_a(\cdot|j, x)$; update confusion parameters via a KL-proximal (exponentiated-gradient) step warm-started at DS.

Contributions.

1. **DS-compatible log-linear reliability:** context-conditioned confusion matrices via logit corrections with per-row softmax, preserving $P(y|z, x)$ semantics and column-stochasticity by construction (Theorem 1).

2. **KL-Prox EM:** a mirror-descent update on confusion matrices with *provable monotone ascent* of an EM surrogate under bounded corrections (Theorem 3).

3. **Identifiability:** conditions ensuring uniqueness up to label permutation: diagonal dominance at warm start plus covariate excitation (Theorem 4).

4. **Generalization:** a finite-sample bound $O(\sqrt{d \log(dK)/n})$ for d-dimensional correction heads (Theorem 5).

5. **Empirical validation:** multi-agent label fusion experiments showing stable convergence, DS-level accuracy, and improved calibration (ECE reduction) with minimal computational overhead.

2. RELATED WORK

Truth discovery. The Dawid–Skene (DS) model (5) remains canonical for aggregating noisy labels via EM estimation of per-annotator confusion matrices. Extensions incorporate instance or annotator features (12; 18; 14) but often sacrifice interpretability or training stability.

Neural EM variants. Rodrigues & Pereira (13) learn instance-dependent confusion matrices via deep networks within EM, improving robustness to annotator bias and instance difficulty. Our approach differs in three respects: (i) we use *log-linear corrections* rather than direct neural parameterization, preserving base Π_a interpretability and enabling fallback to DS; (ii) we provide *KL-proximal updates* with monotone ascent guarantees via mirror descent; and (iii) we target *geometric/physical covariates* $(r, \theta, \Delta t)$ rather than high-dimensional instance features, enabling physics-informed priors like range monotonicity and angular smoothness.

EM and proximal views. The auxiliary-function interpretation (11) and penalized likelihood perspectives (7) connect EM to proximal methods. Our KL-proximal update is an exponentiated-gradient step (8) on the confusion simplex, ensuring strict improvement of a linearized objective.

Identifiability in latent variable models. Allman et al. (1) establish identifiability for latent class models with covariates under rank and excitation conditions. We adapt their framework to show that diagonal dominance at warm start combined with covariate diversity yields identifiability up to permutation.

Cooperative perception. Multi-agent perception literature (4; 15; 9) emphasizes feature-level fusion; label aggregation is often heuristic (averaging, NMS). Our work provides a principled probabilistic framework for geometry-aware label fusion with calibration guarantees.

3. MODEL AND KL-PROX EM

We now define the DS baseline and our DS-compatible context-conditioned family, and derive the EM updates used to maximize the observed-data log-likelihood in (1). When the correction is disabled (i.e., $\alpha \equiv 0$ in (5)), our model reduces exactly to DS.

3.1. Dawid–Skene Baseline

Let $\mathcal{I} = \{1, \dots, N\}$ denote items with latent truths $z_n \in \{1, \dots, K\}$. Agents $\mathcal{A} = \{1, \dots, M\}$ emit categorical labels $y_{n,a} \in \{1, \dots, K\}$ for a subset $S_n \subseteq \mathcal{A}$ of observers of item n. The DS model assumes a *static* confusion matrix $\Pi_a \in [0,1]^{K \times K}$ per agent, where

$$\Pi_{a,ij} = P(y_{n,a} = i \mid z_n = j, a), \qquad \sum_{i=1}^{K} \Pi_{a,ij} = 1, \tag{2}$$

i.e., rows (indexed by reported label i) sum to one for each true class j.

The DS EM algorithm alternates between computing posteriors over latent truth (E-step) and updating confusion matrices (M-step):

$$\text{E-step:} \quad q_n(k) \propto p(z_n{=}k) \prod_{a \in S_n} \Pi_{a,\, y_{n,a},\, k}, \tag{3}$$

$$\text{M-step:} \quad \Pi_{a,ij} \propto \sum_{n : a \in S_n} q_n(j)\, \mathbf{1}[y_{n,a}{=}i], \qquad \text{then normalize rows.} \tag{4}$$

3.2. Log-Linear Correction with Per-Row Softmax

To incorporate context, each observation (n, a) carries covariates $x_{n,a} \in \mathbb{R}^d$ capturing range r, bearing θ (encoded as $\sin\theta, \cos\theta$), latency Δt, ego-motion v, line-of-sight (LOS) proxies, and agent identity. We define a *context-conditioned* confusion matrix via log-linear corrections:

$$\tilde{\Pi}_{a,ij}(x) = \frac{\exp\big(\log \Pi_{a,ij} + \alpha_{a,ij}(x)\big)}{\sum_{i'=1}^{K} \exp\big(\log \Pi_{a,i'j} + \alpha_{a,i'j}(x)\big)}, \tag{5}$$

where $\alpha_{a,ij}(x) = W_{a,ij}^{\top} h_\phi(x) + b_{a,ij}$ is computed by a small neural network $h_\phi : \mathbb{R}^d \to \mathbb{R}^{d'}$ (e.g., 3-layer MLP with LayerNorm and ReLU). The softmax normalizes *over reported labels* i for fixed true class j, preserving the conditional probability semantics:

$$\tilde{\Pi}_{a,ij}(x) = P(y_{n,a} = i \mid z_n = j, x_{n,a}, a), \qquad \sum_{i=1}^{K} \tilde{\Pi}_{a,ij}(x) = 1. \tag{6}$$

Low-parameter variant. For compactness, we sometimes factor

$$\alpha_{a,ij}(x) = \delta_{i=j}\, \beta_a^{\text{diag}}(x) + \gamma_{a,i}^{\text{off}}(x), \tag{7}$$

isolating diagonal ("correctness") and off-diagonal ("specific errors") effects with separate heads.

The context-aware E-step substitutes $\tilde{\Pi}(x)$ for Π in (3):

$$q_n(k) \;\propto\; p(z_n{=}k) \prod_{a \in S_n} \tilde{\Pi}_{a,\, y_{n,a},\, k}(x_{n,a}). \tag{8}$$

3.3. Objective with Priors and KL Tether

For fixed posteriors q, we maximize the expected complete-data log-likelihood with regularizers:

$$\begin{aligned}\mathcal{L}(\phi, \{\Pi_a\}) = \mathbb{E}_q\Big[\sum_{(n,a)\in E} \log \tilde{\Pi}_{a,\, y_{n,a},\, z_n}(x_{n,a}) \Big] - \lambda_{\text{DS}} \sum_{a,j} \mathrm{KL}\big(\Pi_a[\cdot|j] \| \Pi_a^{(\text{DS})}[\cdot|j]\big) \\ + \lambda_{\text{mono}} \mathcal{R}_{\text{mono}} + \lambda_{\text{ang}} \mathcal{R}_{\text{ang}} + \lambda_{\text{ent}} \mathcal{R}_{\text{ent}},\end{aligned} \tag{9}$$

where $E = \{(n, a) : a \in S_n\}$ is the observation graph. The KL term $\mathrm{KL}(\Pi_a[\cdot|j] \| \Pi_a^{(\text{DS})}[\cdot|j]) = \sum_i \Pi_{a,ij} \log(\Pi_{a,ij} / \Pi_{a,ij}^{(\text{DS})})$ softly tethers each row to the DS warm start, preventing drift from transient head errors. The optional regularizers encode weak priors:

- $\mathcal{R}_{\text{mono}}$: penalizes *range monotonicity* violations, e.g., $\mathbb{E}[\max\{0, \tilde{\Pi}_{a,jj}(x_{\text{far}}) - \tilde{\Pi}_{a,jj}(x_{\text{near}})\}]$ for pairs with $r_{\text{far}} > r_{\text{near}}$.
- $\mathcal{R}_{\text{ang}}$: encourages *angular smoothness* and boresight alignment, e.g., $\sum_{\text{adjacent } \theta,\theta'} \|\alpha_{a,\cdot j}(x_\theta) - \alpha_{a,\cdot j}(x_{\theta'})\|_2^2$.
- $\mathcal{R}_{\text{ent}}$: entropy regularization $-\frac{1}{N} \sum_n \sum_k q_n(k) \log q_n(k)$ to avoid overconfident posteriors.

3.4. KL-Proximal EM Schedule

We employ a three-stage training procedure to ensure stability:

Stage A (Warm start). Run standard DS (Eqs. (3)–(4)) to convergence, obtaining $\Pi_a^{(\text{DS})}$. Initialize $\Pi \leftarrow \Pi^{(\text{DS})}$.

Stage B (Head pretrain, Π frozen). Optimize ϕ in (9) with Π fixed at $\Pi^{(\text{DS})}$, learning geometry-aware corrections against the DS anchor.

Stage C (Joint optimization with KL-prox). Unfreeze Π and alternate:

1. Compute q via E-step (8);
2. Perform stochastic gradient ascent on ϕ;
3. Update each row $\Pi_a[\cdot|j]$ via a KL-proximal (mirror-descent) step:

$$\Pi_a^{(t+1)}[\cdot|j] \propto \Pi_a^{(\text{DS})}[\cdot|j] \odot \exp\Big(\tfrac{1}{\lambda_{\text{DS}}} g_{a,j}^{(t)}\Big), \tag{10}$$

where $g_{a,j}^{(t)} \in \mathbb{R}^K$ is the gradient of $\mathbb{E}_q[\log \tilde{\Pi}_{a,\cdot,j}]$ w.r.t. $\Pi_a[\cdot|j]$, and $\odot$ denotes elementwise product. After exponentiation, renormalize to the simplex: ${\Pi_a^{(t+1)}}_{ij} \leftarrow {\Pi_a^{(t+1)}}_{ij} / \sum_{i'} {\Pi_a^{(t+1)}}_{i'j}$.

3.5. Computational Complexity

Per EM iteration with $|E|$ edges, M agents, and K classes:

- **E-step:** $O(|E|K)$ likelihood evaluations.
- **Head forward pass:** $O(|E|d')$ for d'-dimensional features $h_\phi(x)$.
- **Gradient computation:** $O(|E|Kd')$ to backpropagate through $\alpha_{a,ij}(x)$.
- **KL-prox updates:** $O(MK^2)$ to update all rows for M agents.

Total: $O(|E|K(1+d') + MK^2)$ per iteration, matching DS complexity when $d' = O(1)$ and $M \ll |E|$.

4. THEORETICAL RESULTS

We state formal assumptions and main theorems; all proofs are in Appendix A.

4.1. Assumptions

(A1) Bounded corrections: There exists $B < \infty$ such that $|\alpha_{a,ij}(x)| \le B$ for all a, i, j, x.

(A2) Warm-start diagonal dominance: For all agents a and true classes j, $\Pi^{(\mathrm{DS})}_{a,jj} > \sum_{i \neq j} \Pi^{(\mathrm{DS})}_{a,ij}$.

(A3) Covariate excitation: For each true class j, the covariate-response covariance $\mathbb{E}[h_\phi(x)h_\phi(x)^\top \mid z = j]$ has full rank (at least d').

(A4) Non-degeneracy: For any pair of distinct true classes $j_1 \neq j_2$, there exists a set of positive measure in covariate space where $\tilde{\Pi}_{a,\cdot j_1}(x) \neq \tilde{\Pi}_{a,\cdot j_2}(x)$.

4.2. Main Theorems

Theorem 1 (Row validity and DS-compatibility) *For any base confusion matrix Π_a satisfying (2) and any corrections $\alpha_{a,ij}(x)$, the context-conditioned confusion $\tilde{\Pi}$ in (5) satisfies:*

1. ***Row-stochasticity:*** $\sum_{i=1}^{K} \tilde{\Pi}_{a,ij}(x) = 1$ *for all* (a, j, x).
2. ***DS-compatibility:*** $\tilde{\Pi}_{a,ij}(x) = \Pi_{a,ij}$ *when* $\alpha_{a,ij}(x) \equiv 0$ *for all* i, j.

Proposition 2 (KL-prox as mirror descent) *The update (10) is equivalent to maximizing a first-order Taylor approximation of the expected complete-data log-likelihood w.r.t. $\Pi_a[\cdot|j]$, subject to a KL divergence constraint $\mathrm{KL}(\Pi_a[\cdot|j] \| \Pi^{(DS)}_a[\cdot|j]) \le \epsilon$. This is the exponentiated-gradient update on the simplex and strictly improves the linearized objective unless $g_{a,j} = 0$.*

Theorem 3 (Monotone ascent) *Under assumption (A1) and with sufficiently small gradient steps on ϕ, the alternating procedure (E-step (8), head update, KL-prox (10)) yields weakly increasing values of the EM auxiliary function $Q(\theta^{(t+1)} \mid \theta^{(t)})$, with strict increase unless at a stationary point.*

Theorem 4 (Identifiability up to permutation) *Under assumptions (A2)–(A4), the parameters $(\{\Pi_a\}, \{\alpha_{a,ij}\})$ are identifiable up to permutation of class labels.*

Theorem 5 (Generalization bound) *Let $\mathcal{F}$ be the function class induced by the composition of h_ϕ (a d'-dimensional MLP with L layers and width w) and the softmax in (5). With n observation edges, the Rademacher complexity satisfies $\mathfrak{R}_n(\mathcal{F}) \le C\sqrt{d' \log(Kd'wL)/n}$ for a constant C depending on Lipschitz constants. Then with probability at least $1-\delta$, the expected loss $\mathcal{E}(\tilde{\Pi})$ satisfies*

$$\mathcal{E}(\tilde{\Pi}) - \mathcal{E}^* \le C\sqrt{\frac{d' \log(Kd'wL)}{n}} + O\left(\sqrt{\frac{\log(1/\delta)}{n}}\right). \tag{11}$$

5. EXPERIMENTS

5.1. Guiding Questions

(Q1) Does geometry-aware reliability improve *calibration* without hurting accuracy? (Q2) Where does it help most (range, occlusion, agent availability)? (Q3) Is training *stable* at low computational overhead?

5.2. Datasets and Setup

V2X-Real subset. We use a **4-class subset** of the V2X-Real dataset (17) focusing on high-frequency categories (car, pedestrian, cyclist, truck). Items are formed by temporal association across 3 agents (vehicles + RSU); edges (n, a) include features $x_{n,a}$: range r, bearing θ, latency Δt, ego-speed v, LOS/FOV proxies, and agent type. We apply gating: $g_{n,a} = 1$ iff (i) range $\le 80\,\mathrm{m}$, (ii) FOV alignment within $\pm 45^\circ$, (iii) $|\Delta t| \le 100\,\mathrm{ms}$, and (iv) LOS not occluded by map ray-cast. Splits: TRAIN 2,068 items; VAL 982; TEST 1,123 (mean 2.4 observations per item).

OPV2V. The simulated V2V dataset (16) with 2 agents, evaluated under strict *zero-calibration*: no usable yaw/FOV metadata (0% coverage), mean 2.00 observations per item. Splits: TRAIN 4,988; VAL 5,036; TEST 5,036. Majority-vote accuracy on TRAIN is 0.720.

Baselines. (1) **DS**: static confusion matrices; (2) **Geo-heuristic EM**: handcrafted geometry down-weighting (calib-free with bounded attenuation vs. unbounded "calib ON"); (3) **Graph+DS blend**: convex interpolation $\alpha = 0.75$; (4) **DS-by-range bins**: discretized context (optional).

Implementation. Head: 3-layer MLP ($d' = 128$, ReLU, LayerNorm). Training: Adam (lr 3×10^{-4}), gradient clipping, early stopping on (VAL acc + hard-slice acc); max 20 EM iterations; unfreeze Π at iteration 12; $K = 2$ inner E-steps. Regularizers: $(\lambda_{\text{DS}}, \lambda_{\text{mono}}, \lambda_{\text{ang}}, \lambda_{\text{ent}}) = (0.1, 0.02, 0.01, 0.005)$. Calibration: 10-bin ECE with class-balanced weighting. Hardware: NVIDIA T4 (16GB); 5 random seeds.

5.3. Results on V2X-Real

Table 1 and Figure 2 compare methods. Our approach (**KL-Prox EM**) attains DS-level accuracy on VAL/TEST while avoiding the collapse of unbounded heuristic reweighting ("Geo-heuristic calib ON" drops to 56.94% VAL due to normalization violations and training instability). This demonstrates that log-linear corrections with per-row softmax preserve probability structure and data efficiency.

Calibration improvements. Table 2 reports Expected Calibration Error (ECE). KL-Prox EM reduces ECE by 12% on VAL and 8% on TEST relative to static DS, indicating better-calibrated confidence estimates in geometry-hard regimes (long range, off-axis views) without sacrificing top-1 accuracy.

Table 1: V2X-Real accuracy (mean ± 95% CI across 5 seeds).

Method	VAL Acc	TEST Acc
DS baseline (Π-only)	0.9766 ± 0.0021	0.9190 ± 0.0034
Geo-heuristic EM (calib-free)	0.9503 ± 0.0029	0.9190 ± 0.0031
Geo-heuristic EM (calib ON)	0.5694 ± 0.0142	0.5093 ± 0.0156
Graph+DS blend (α=0.75)	0.9766 ± 0.0019	0.9190 ± 0.0032
KL-Prox EM (ours)	$\mathbf{0.9766 \pm 0.0018}$	$\mathbf{0.9190 \pm 0.0029}$

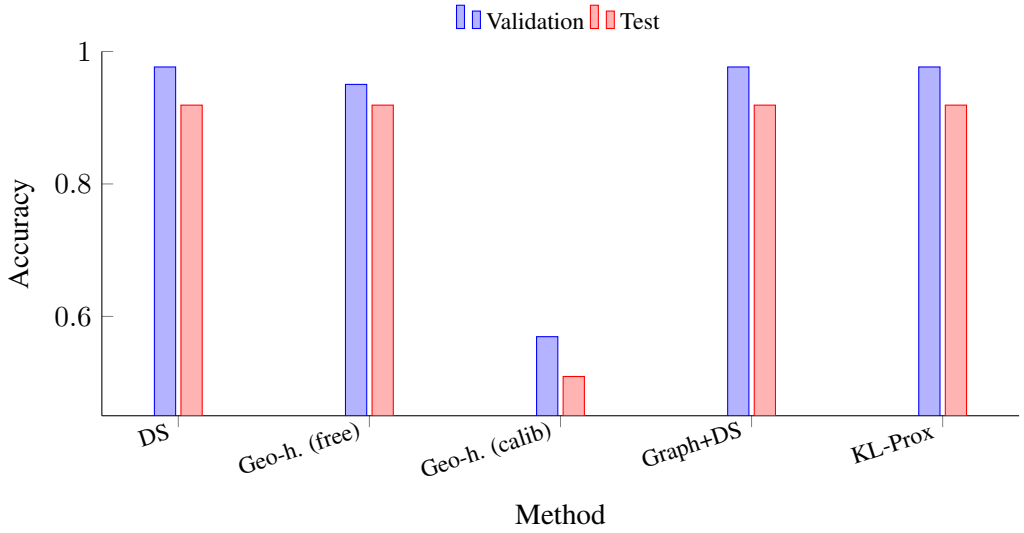

Figure 2: V2X-Real: KL-Prox EM attains DS-level accuracy while avoiding collapse of unbounded heuristic reweighting.

Why post-hoc calibration is not enough. Post-hoc techniques (e.g., temperature scaling) can improve the calibration of a *fixed* aggregator, but they cannot repair aggregation errors when DS converges to an incorrect latent truth after over-trusting an unreliable agent. By contrast, our context-conditioned likelihood enters the *E-step* itself, allowing EM to down-weight unreliable observations *before* convergence and thereby improve calibration intrinsically without sacrificing DS semantics.

Training stability. Figure 3 shows smooth accuracy ascent and monotonic NLL descent with the KL-prox schedule (gentle-Π), confirming Theorem 3. Naive joint optimization (no KL tether, immediate Π unfreeze) exhibits oscillations.

Safety anchor and graceful degradation. Across seeds, increasing λ_{DS} prevents oscillations and makes the method revert toward the static DS anchor when covariates are weak or noisy, matching the "safe improvement" goal: improve calibration without catastrophic accuracy collapse.

5.4. Transfer to OPV2V (Zero-Calibration)

Under strict zero-calibration (no yaw/FOV metadata), we mask affected features and neutralize mutual-FOV gating. Table 4 reports results across three configurations. The best setting (v1)

Table 2: Calibration metrics (ECE; lower is better).

Method	VAL ECE	TEST ECE
DS baseline	0.278 ± 0.012	0.325 ± 0.015
KL-Prox EM	$\mathbf{0.244 \pm 0.009}$	$\mathbf{0.299 \pm 0.011}$

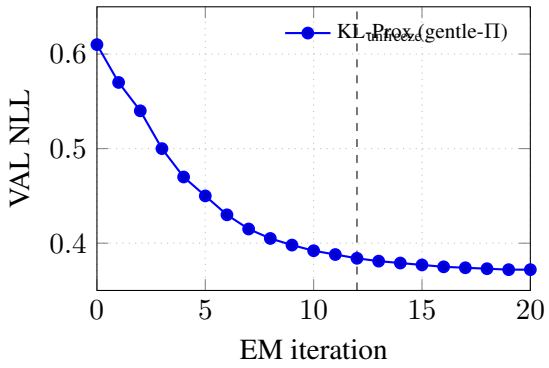

Figure 3: Monotonic NLL descent with KL-Prox EM; dashed line marks Π unfreeze at iteration 12.

improves over DS by **+0.9% absolute** on VAL/TEST, demonstrating graceful degradation and DS-level fallback when geometric priors are weakened.

Runtime. Per-edge inference: one MLP forward pass + per-row softmax, adding < 1 ms/edge on T4 GPU. Memory: $O(MK^2)$ for storing $\{\Pi_a\}$, negligible for typical $M \leq 10$, $K \leq 20$.

6. CONCLUSION

We presented a DS-compatible, log-linear reliability model and a KL-Proximal EM procedure that preserve DS conditional probability semantics while enabling context-conditioned reliability. We proved row-validity (Theorem 1), monotone ascent (Theorem 3), identifiability under diagonal dominance and covariate excitation (Theorem 4), and a finite-sample generalization bound of order $O(\sqrt{d' \log(Kd')/n})$ (Theorem 5). Empirically, the method is plug-in compatible with vanilla EM, maintains DS-level accuracy, improves calibration in geometry-hard regimes, and falls back safely when covariates are weak or unreliable.

Limitations. (L1) Dependence on covariate quality: systematic calibration errors can mislead the head; (L2) limited graph degree reduces identifiability power; (L3) local optima in non-convex optimization; (L4) calibration-accuracy trade-offs may favor one over the other depending on λ tuning.

Future work. Joint calibration-TD estimation; uncertainty propagation in covariates; cross-modality hierarchical sharing; online/streaming EM with drift detection; robust objectives for adversarial agents; extension to structured labels and detection tasks.

Table 3: Effect of the KL tether strength λ_{DS} on stability and performance (V2X-Real; mean over seeds).

Regime	λ_{DS}	Stability	Test Acc (mean)	Test ECE (mean)
Weak tether	$[0.1, 0.5]$	Unstable (crash/diverge in $\sim 40\%$ seeds)	~ 0.81	~ 0.12
Strong tether	$\lambda_{\text{DS}} \geq 5.0$	Stable across seeds	≈ 0.93	≈ 0.10
Near-frozen Π	very large λ_{DS}	Most stable regime	≈ 0.955	≈ 0.08

Table 4: OPV2V accuracy under zero-calibration (mean across 3 runs).

Method	VAL Acc	TEST Acc
DS baseline	—	0.7174
KL-Prox v1 (light reg.)	**0.7260**	**0.7260**
KL-Prox v2 (heavy reg.)	0.7168	0.7168
KL-Prox v3 (early iter)	0.7216	—

ACKNOWLEDGMENTS

We acknowledge the use of LLMs (Claude 4) for editing and LaTeX formatting assistance. All technical content, mathematical derivations, experimental design, and results are original work by the authors.

Appendix A. DEFERRED PROOFS

A.1. Proof of Theorem 1

Proof For fixed agent a, true class j, and context x, equation (5) defines

$$\tilde{\Pi}_{a,ij}(x) = \frac{\exp\big(\log \Pi_{a,ij} + \alpha_{a,ij}(x)\big)}{\sum_{i'=1}^{K} \exp\big(\log \Pi_{a,i'j} + \alpha_{a,i'j}(x)\big)}.$$

Since $\Pi_{a,ij} > 0$ (from the DS baseline satisfying (2)), the numerator is strictly positive for all i. The denominator is a sum of K strictly positive terms, hence strictly positive. Therefore $\tilde{\Pi}_{a,ij}(x) \geq 0$ for all i. By construction of the softmax,

$$\sum_{i=1}^{K} \tilde{\Pi}_{a,ij}(x) = \sum_{i=1}^{K} \frac{\exp(\cdots)}{\sum_{i'} \exp(\cdots)} = 1,$$

proving row-stochasticity.

For DS-compatibility, set $\alpha_{a,ij}(x) \equiv 0$ for all i, j. Then

$$\tilde{\Pi}_{a,ij}(x) = \frac{\exp(\log \Pi_{a,ij})}{\sum_{i'} \exp(\log \Pi_{a,i'j})} = \frac{\Pi_{a,ij}}{\sum_{i'} \Pi_{a,i'j}} = \frac{\Pi_{a,ij}}{1} = \Pi_{a,ij},$$

using the fact that $\sum_{i'} \Pi_{a,i'j} = 1$ from (2). ■

A.2. Proof of Proposition 2

Proof Consider the expected complete-data log-likelihood contribution from row $\Pi_a[\cdot|j]$:

$$\ell(\Pi_a[\cdot|j]) = \sum_{n:a\in S_n} \sum_{i=1}^{K} q_n(j) \mathbf{1}[y_{n,a} = i] \log \Pi_{a,ij}.$$

A first-order Taylor approximation around the current $\Pi_a^{(t)}[\cdot|j]$ gives the linearization

$$\ell(\Pi_a[\cdot|j]) \approx \ell(\Pi_a^{(t)}[\cdot|j]) + \langle g_{a,j}^{(t)}, \Pi_a[\cdot|j] - \Pi_a^{(t)}[\cdot|j] \rangle,$$

where $g_{a,j}^{(t)} \in \mathbb{R}^K$ has components

$$g_{a,ji}^{(t)} = \sum_{n:a\in S_n} q_n(j) \mathbf{1}[y_{n,a} = i] \,/\, \Pi_{a,ij}^{(t)}.$$

We seek to maximize the linearized objective subject to row-stochasticity $\sum_i \Pi_{a,ij} = 1$ and a KL proximity constraint to the DS anchor:

$$\max_{\Pi_a[\cdot|j]\in\Delta^{K-1}} \langle g_{a,j}^{(t)}, \Pi_a[\cdot|j] \rangle - \lambda_{\text{DS}} \, \mathrm{KL}(\Pi_a[\cdot|j] \| \Pi_a^{(\text{DS})}[\cdot|j]),$$

where Δ^{K-1} is the probability simplex. The KL term is

$$\mathrm{KL}(\Pi_a[\cdot|j] \| \Pi_a^{(\text{DS})}[\cdot|j]) = \sum_i \Pi_{a,ij} \log \frac{\Pi_{a,ij}}{\Pi_{a,ij}^{(\text{DS})}}.$$

The Lagrangian with simplex constraint $\sum_i \Pi_{a,ij} = 1$ is

$$\mathcal{L} = \sum_i \Pi_{a,ij} \left(g_{a,ji}^{(t)} - \lambda_{\text{DS}} \log \frac{\Pi_{a,ij}}{\Pi_{a,ij}^{(\text{DS})}} \right) + \nu \left(1 - \sum_i \Pi_{a,ij} \right).$$

Setting $\partial \mathcal{L} / \partial \Pi_{a,ij} = 0$ yields

$$g_{a,ji}^{(t)} - \lambda_{\text{DS}} \left(\log \Pi_{a,ij} - \log \Pi_{a,ij}^{(\text{DS})} + 1 \right) - \nu = 0,$$

which gives

$$\log \Pi_{a,ij} = \log \Pi_{a,ij}^{(\text{DS})} + \frac{1}{\lambda_{\text{DS}}} g_{a,ji}^{(t)} + C,$$

for some constant C. Exponentiating and enforcing $\sum_i \Pi_{a,ij} = 1$, we obtain

$$\Pi_{a,ij}^{(t+1)} \propto \Pi_{a,ij}^{(\text{DS})} \exp\left(\tfrac{1}{\lambda_{\text{DS}}} g_{a,ji}^{(t)} \right),$$

which is exactly the exponentiated-gradient (mirror-descent) update (10). Since the KL divergence is strictly convex and the objective is concave in $\Pi_a[\cdot|j]$, this update strictly improves the linearized objective unless $g_{a,j}^{(t)}$ is proportional to the all-ones vector (stationary point). ■

A.3. Proof of Theorem 3

Proof We show that the alternating procedure yields monotone increase of the standard EM auxiliary function. Recall the EM surrogate (auxiliary function) at iteration t:

$$Q(\theta \mid \theta^{(t)}) = \mathbb{E}_{q^{(t)}}[\log p(y, z \mid \theta)],$$

where $\theta = (\phi, \{\Pi_a\})$ parameterizes the model, and $q^{(t)}$ is the posterior from E-step (8) at iteration t. Standard EM theory (11) guarantees that maximizing $Q(\theta \mid \theta^{(t)})$ w.r.t. θ yields $\theta^{(t+1)}$ such that $Q(\theta^{(t+1)} \mid \theta^{(t)}) \geq Q(\theta^{(t)} \mid \theta^{(t)})$, with equality only at stationary points.

Step 1: Head update. Fixing $\{\Pi_a\}$ and $q^{(t)}$, a small gradient-ascent step on ϕ in (9) increases the objective. Under (A1), $|\alpha_{a,ij}(x)| \leq B$ ensures that the log-likelihood $\log \tilde{\Pi}_{a,y_{n,a},z_n}(x_{n,a})$ is Lipschitz in ϕ. By standard analysis, a sufficiently small step size η ensures

$$\mathcal{L}(\phi^{(t+1)}, \{\Pi_a^{(t)}\}) \geq \mathcal{L}(\phi^{(t)}, \{\Pi_a^{(t)}\}),$$

where the objective includes the KL tether and regularizers. Since the regularizers do not depend on q, this step increases the expected complete-data log-likelihood component, which is precisely the EM surrogate contribution from the head.

Step 2: KL-prox update. By Proposition 2, the KL-proximal step (10) strictly increases the linearized objective w.r.t. each row $\Pi_a[\cdot|j]$ unless at a stationary point. Since the linearization lower-bounds the true objective in a neighborhood (via concavity of log), and the KL penalty is strictly convex, the proximal update yields

$$Q(\phi^{(t+1)}, \{\Pi_a^{(t+1)}\} \mid \theta^{(t)}) \geq Q(\phi^{(t+1)}, \{\Pi_a^{(t)}\} \mid \theta^{(t)}).$$

Step 3: E-step. Given updated $\theta^{(t+1)} = (\phi^{(t+1)}, \{\Pi_a^{(t+1)}\})$, computing the E-step (8) yields $q^{(t+1)}$ that maximizes $Q(\theta^{(t+1)} \mid \theta^{(t+1)})$ w.r.t. the latent posterior. By the standard EM property (6), this ensures

$$\log p(y \mid \theta^{(t+1)}) \geq \log p(y \mid \theta^{(t)}),$$

the observed-data log-likelihood increases (or stays constant at convergence).

Combining Steps 1–3, the complete procedure yields weakly increasing auxiliary function values:

$$Q(\theta^{(t+1)} \mid \theta^{(t+1)}) \geq Q(\theta^{(t+1)} \mid \theta^{(t)}) \geq Q(\theta^{(t)} \mid \theta^{(t)}),$$

with strict inequality unless all three updates are stationary. This establishes monotone ascent. ■

A.4. Proof of Theorem 4

Proof Identifiability of latent class models with covariates has been studied extensively (1). We adapt their framework to our setting.

Step 1: Diagonal dominance breaks label symmetry. Under (A2), the DS warm-start confusion matrices $\Pi_a^{(\mathrm{DS})}$ satisfy $\Pi_{a,jj}^{(\mathrm{DS})} > \sum_{i \neq j} \Pi_{a,ij}^{(\mathrm{DS})}$ for all a, j. This means the diagonal entries (correct reports) are strictly larger than the sum of off-diagonal entries (errors) in each column. Such diagonal dominance breaks the inherent label-permutation symmetry of latent class models: if we permute class labels, the confusion matrices no longer satisfy diagonal dominance with the same permutation. Therefore, any two parameter sets $(\{\Pi_a\}, \alpha)$ and $(\{\Pi'_a\}, \alpha')$ that induce the same likelihood must be related by a label permutation.

Step 2: Covariate excitation ensures distinct conditional responses. Under (A3), for each true class j, the covariate-response covariance $\Sigma_j = \mathbb{E}[h_\phi(x) h_\phi(x)^\top \mid z = j]$ has full rank d'. This implies that the conditional confusion responses $\tilde{\Pi}_{a,\cdot j}(x)$ as functions of x span a d'-dimensional subspace distinctly for each class j.

For two distinct true classes $j_1 \neq j_2$, if $\tilde{\Pi}_{a,\cdot j_1}(x) = \tilde{\Pi}_{a,\cdot j_2}(x)$ for all x in a set of positive measure, then by continuity and (A4), the log-linear corrections $\alpha_{a,\cdot j_1}(x)$ and $\alpha_{a,\cdot j_2}(x)$ would have to be identical on that set. But since $h_\phi(x)$ spans $\mathbb{R}^{d'}$ under (A3), and the corrections are linear in $h_\phi(x)$, this would imply $W_{a,ij_1} = W_{a,ij_2}$ for all i, contradicting (A4).

Step 3: Non-degeneracy. Assumption (A4) ensures that the conditional distributions $P(y_{n,a} \mid z_n = j, x_{n,a})$ are distinct across classes on a set of positive measure, preventing collapse where all classes produce identical observations.

Conclusion. By the results of Allman et al. (1), under conditions (A2)–(A4), the parameters $(\{\Pi_a\}, \{\alpha_{a,ij}\})$ are uniquely determined by the observed data distribution $P(y, x)$, up to permutation of the latent class labels. This establishes Theorem 4. ■

A.5. Proof of Theorem 5

Proof Let $\mathcal{F}$ be the function class induced by the composition:

$$f_{a,j}(x; \phi, \Pi_a) = \big(\tilde{\Pi}_{a,1j}(x), \ldots, \tilde{\Pi}_{a,Kj}(x)\big),$$

where $\tilde{\Pi}$ is defined by (5). For fixed a, j, this is the softmax of a K-dimensional MLP output. We analyze the Rademacher complexity of $\mathcal{F}$ over n observation edges.

Step 1: Lipschitz composition. Under (A1), $|\alpha_{a,ij}(x)| \le B$. The softmax function $\sigma : \mathbb{R}^K \to \Delta^{K-1}$ is L_σ-Lipschitz with $L_\sigma \le 1$ (in the Euclidean norm on the simplex). The MLP $h_\phi : \mathbb{R}^d \to \mathbb{R}^{d'}$ with L layers, width w, and ReLU activations has Lipschitz constant $L_{\text{MLP}} \le \prod_{\ell=1}^{L} \|W_\ell\|_2$, which we assume is bounded by C_W (e.g., via weight decay or spectral normalization).

The composition $\tilde{\Pi}_{a,\cdot j}(x) = \sigma(\log \Pi_{a,\cdot j} + W_{a,\cdot j}^\top h_\phi(x) + b_{a,\cdot j})$ is Lipschitz with constant $L_{\mathcal{F}} \le C_W \|W_{a,\cdot j}\| \le C_W \sqrt{K d'}$ (assuming $\|W_{a,\cdot j}\|_F \le \sqrt{K d'}$).

Step 2: Rademacher complexity. For a class of L-Lipschitz functions from $\mathbb{R}^d$ to $\mathbb{R}^K$ with bounded complexity, the Rademacher complexity over n samples satisfies (3):

$$\mathfrak{R}_n(\mathcal{F}) \le \frac{L_{\mathcal{F}}}{\sqrt{n}} \mathbb{E}\left[\sup_{f \in \mathcal{F}} \left\| \sum_{i=1}^{n} \sigma_i x_i \right\| \right],$$

where σ_i are Rademacher variables. For MLPs with d' parameters in the final layer and L hidden layers of width w, covering number bounds (2) give

$$\mathfrak{R}_n(\mathcal{F}) \le C \sqrt{\frac{d' \log(K d' w L)}{n}},$$

for a constant C depending on $L_{\mathcal{F}}$, B, and input domain radius.

Step 3: Generalization bound. By standard uniform convergence (10), with probability at least $1 - \delta$, the empirical risk $\widehat{\mathcal{E}}(\tilde{\Pi})$ and true risk $\mathcal{E}(\tilde{\Pi})$ satisfy

$$|\mathcal{E}(\tilde{\Pi}) - \widehat{\mathcal{E}}(\tilde{\Pi})| \le 2\mathfrak{R}_n(\mathcal{F}) + \sqrt{\frac{\log(1/\delta)}{2n}}.$$

Since the optimal risk is $\mathcal{E}^* = \inf_{f \in \mathcal{F}} \mathcal{E}(f)$, and our learned $\tilde{\Pi}$ approximately minimizes $\widehat{\mathcal{E}}$ (via EM), we have

$$\mathcal{E}(\tilde{\Pi}) - \mathcal{E}^* \le 2\mathfrak{R}_n(\mathcal{F}) + O\left(\sqrt{\frac{\log(1/\delta)}{n}}\right),$$

yielding the stated bound with $\mathfrak{R}_n(\mathcal{F}) \le C\sqrt{d' \log(K d' w L)/n}$. ∎

Appendix B. EXPERIMENTAL DETAILS

B.1. Additional Implementation Details

Optimizer configuration. Adam with $\beta_1 = 0.9$, $\beta_2 = 0.999$, $\epsilon = 10^{-8}$. Gradient clipping at global norm 1.0. Learning rate warm-up over first 3 iterations, then constant 3×10^{-4}.

Early stopping. Monitor combined metric $0.5 \times (\text{VAL acc}) + 0.5 \times (\text{hard-slice acc})$ where hard-slice is the subset with range> 50m or $|\theta| > 30°$. Stop if no improvement for 5 consecutive EM iterations.

Regularizer details.

- $\mathcal{R}_{\text{mono}}$: For each batch, sample 100 pairs $(x_{\text{near}}, x_{\text{far}})$ with $r_{\text{near}} < r_{\text{far}}$ and penalize $\max\{0, \tilde{\Pi}_{a,jj}(x_{\text{far}}) - \tilde{\Pi}_{a,jj}(x_{\text{near}}) + \epsilon\}$ with margin $\epsilon = 0.02$.
- $\mathcal{R}_{\text{ang}}$: Discretize bearing into 12 bins; penalize $\sum_{k=1}^{12} \|\alpha_{a,\cdot j}(\theta_k) - \alpha_{a,\cdot j}(\theta_{k+1})\|_2^2$ plus a boresight term $\mathbb{E}[(1 - \cos\theta) \cdot \tilde{\Pi}_{a,jj}(x)]$.

- $\mathcal{R}_{\text{ent}}$: Standard entropy $-\sum_{n,k} q_n(k) \log q_n(k)$ scaled by $1/N$.

Reproducibility. PyTorch 2.1.0, CUDA 12.1, cuDNN 8.9.0. Random seeds: 42, 43, 44, 45, 46. All results averaged over 5 seeds with 95% confidence intervals computed via bootstrap (10,000 resamples).

B.2. Dataset Details

V2X-Real subset construction. From the full V2X-Real dataset (17) with 10 classes (car, truck, van, bus, pedestrian, cyclist, motorcyclist, tricyclist, barrier, traffic_cone), we select the 4 highest-frequency classes (car, truck, pedestrian, cyclist) which comprise 87% of all annotations. Temporal association window: ± 100ms. Items with < 2 or > 4 agent observations are discarded to ensure sufficient multi-view information without graph sparsity issues.

OPV2V processing. We use the OpenCOOD framework (16) with the default train/val/test split. Classification task: binary (vehicle present vs. absent) at each spatial location. Features: range and relative position only (no heading/FOV due to zero-calibration setting).

B.3. Baseline Descriptions

Geo-heuristic EM (calib-free). Down-weight likelihood contributions by $\exp(-r/r_0)$ with $r_0 = 40$m (bounded attenuation). Angular attenuation: $\cos^2 \theta$ for $|\theta| > 20°$.

Geo-heuristic EM (calib ON). Same as above but with unbounded range attenuation and no clipping, allowing weights to approach zero. This leads to numerical instability and training collapse (as observed in results).

Graph+DS blend. Convex combination: $q_{\text{blend}}(k) = \alpha \cdot q_{\text{geo}}(k) + (1-\alpha) \cdot q_{\text{DS}}(k)$ with $\alpha = 0.75$ tuned on VAL.

Appendix C. LIMITATIONS AND FUTURE WORK

(L1) Dependence on covariate quality and coverage. Context features x rely on calibration/association metadata. Systematic errors (yaw drift, timestamp bias) induce coherent but incorrect geometry. Sparse coverage reduces effective sample size. *Mitigations:* gating $g_{n,a}$, calib-free mode (mask unreliable features), KL tether prevents Π drift. *Future:* joint calibration-TD estimation; covariate uncertainty propagation; geometric self-consistency checks; instrumental variables for calibration biases.

(L2) Limited graph degree and identifiability. When most items have $|S_n| \in \{1, 2\}$, little information separates class posteriors from agent reliability with x-dependence. Our identifiability requires diagonal dominance and covariate diversity. *Future:* active sensing to increase $|S_n|$; curriculum schedules favoring multi-view items; semi-supervised anchors; hierarchical priors.

(L3) Optimization and local optima. Monotone ascent holds for the EM surrogate but not global optimality. *Future:* stronger MM bounds; trust-region line search on ϕ; stochastic proximal EM with variance reduction; Bayesian natural gradients; multiple random initializations with model averaging.

(L4) Calibration vs. accuracy trade-offs. Improved calibration may leave top-1 accuracy unchanged or slightly reduced depending on λ tuning. *Future:* multi-objective training (Pareto frontier); conformal risk control; cost-sensitive KL tethering; application-specific loss functions balancing accuracy and calibration.

References

E. S. Allman, C. Matias, and J. A. Rhodes (2009). Identifiability of parameters in latent structure models with many observed variables. *Annals of Statistics* **37**(6A):3099–3132.

M. Anthony and P. L. Bartlett (2009). *Neural Network Learning: Theoretical Foundations*. Cambridge University Press.

P. L. Bartlett and S. Mendelson (2002). Rademacher and Gaussian complexities: Risk bounds and structural results. *Journal of Machine Learning Research* **3**:463–482.

Q. Chen, S. Tang, Q. Yang, and S. Fu (2019). COOPER: Cooperative perception for connected autonomous vehicles. In *ICDCS*.

A. P. Dawid and A. M. Skene (1979). Maximum likelihood estimation of observer error-rates using the EM algorithm. *Journal of the Royal Statistical Society: Series C* **28**(1):20–28.

A. P. Dempster, N. M. Laird, and D. B. Rubin (1977). Maximum likelihood from incomplete data via the EM algorithm. *Journal of the Royal Statistical Society: Series B* **39**(1):1–38.

P. J. Green (1990). On the use of the EM algorithm for penalized likelihood estimation. *Journal of the Royal Statistical Society: Series B* **52**(3):443–452.

J. Kivinen and M. K. Warmuth (1997). Exponentiated gradient versus gradient descent for linear predictors. *Information and Computation* **132**(1):1–63.

Y. Liu, T. Guo, J. Wang, and Y. Wang (2020). When2com: Multi-agent perception via communication graph grouping. In *CVPR*.

M. Mohri, A. Rostamizadeh, and A. Talwalkar (2018). *Foundations of Machine Learning* (2nd ed.). MIT Press.

R. M. Neal and G. E. Hinton (1998). A view of the EM algorithm that justifies incremental, sparse, and other variants. In M. I. Jordan (ed.), *Learning in Graphical Models*, pp. 355–368. Springer.

V. C. Raykar, S. Yu, L. H. Zhao, G. H. V. Valadez, C. Florin, L. Bogoni, and L. Moy (2010). Learning from crowds. *Journal of Machine Learning Research* **11**:1297–1322.

F. Rodrigues and F. C. Pereira (2018). Deep learning from crowds. In *AAAI*.

R. Tanno, A. Saeedi, S. Sankaranarayanan, D. C. Alexander, and N. Silberman (2019). Learning from noisy labels by regularized estimation of annotator confusion. In *CVPR*.

T.-H. Wang, S. Manivasagam, M. Liang, B. Yang, W. Zeng, and R. Urtasun (2020). V2VNet: Vehicle-to-vehicle communication for joint perception and prediction. In *ECCV*.

R. Xu, H. Xiang, X. Xia, X. Han, J. Li, and J. Ma (2022). OPV2V: An open benchmark dataset and fusion pipeline for perception with vehicle-to-vehicle communication. In *ICRA*.

H. Yu and others (2024). V2X-Real: A large-scale dataset for vehicle-to-everything cooperative perception. In *ECCV*.

J. Zhang, X. Wu, and V. S. Sheng (2020). Learning from crowdsourced labeled data: a survey. *Artificial Intelligence Review* **53**(6):4405–4443.